Radiative efficiencies and global warming potentials of agricultural fumigants

Shine, K. P. ORCID: https://orcid.org/0000-0003-2672-9978 and Kang, Y. ORCID: https://orcid.org/0000-0001-9850-3981
(2023) Radiative efficiencies and global warming potentials of agricultural fumigants. Environmental Research Communications, 5 (5). 051007. ISSN 2515-7620 doi: 10.1088/2515-7620/acd511 Available at https://centaur.reading.ac.uk/112038/

ENVIRONMENTAL RESEARCH
COMMUNICATIONS

LETTER • OPEN ACCESS

Radiative efficiencies and global warming potentials of agricultural fumigants

To cite this article: Keith P Shine and Yi Kang 2023 *Environ. Res. Commun.* **5** 051007

Environmental Research Communications

LETTER

Radiative efficiencies and global warming potentials of agricultural fumigants

Keith P Shine* and **Yi Kang**

Department of Meteorology, University of Reading, United Kingdom

* Author to whom any correspondence should be addressed.

E-mail: k.p.shine@reading.ac.uk

Keywords: agricultural fumigants, global warming potential, cyanogen, ethyl formate, hydrogen cyanide, phosphine

Supplementary material for this article is available online

OPEN ACCESS

RECEIVED
7 February 2023

REVISED
18 April 2023

ACCEPTED FOR PUBLICATION
12 May 2023

PUBLISHED
23 May 2023

Abstract

A rounded assessment of the environmental impacts of fumigants used within the agricultural sector must consider the potential climate impacts of their release into the atmosphere. Within policy settings, the 100-year Global Warming Potential (GWP_{100}) is the most commonly used metric. While GWP_{100} values are available for the widely used fumigant sulfuryl fluoride, no estimates are available for 4 alternative fumigants: ethyl formate, cyanogen, hydrogen cyanide and phosphine. Existing laboratory measurements of the infrared spectra and reaction rate coefficients of these gases are used to produce new estimates of their radiative efficiencies and atmospheric lifetimes, and the first estimates of their GWP_{100} and other climate emission metrics. Although uncertainties are considerable, their GWP_{100} values are estimated to be no more than 2% of the GWP_{100} value of sulfuryl fluoride. These new estimates will enable informed estimates of the climate impact of the use of these fumigants, which must account for the differing usage and release rates to achieve the same fumigant efficacy.

1. Introduction

Chemical fumigants are used as pesticides in the agricultural industry. Methyl bromide (CH_3Br) was traditionally widely used but it is being phased out under the terms of the Montreal Protocol on substances that deplete the ozone layer. Atmospheric concentrations of one alternate for methyl bromide, sulfuryl fluoride (SO_2F_2), are rapidly increasing (Gressent *et al* 2021) despite concerns overs its high (more than 4500) 100-year global warming potential (GWP_{100}) (Papadimitriou *et al* 2008).

Several alternative fumigants have been proposed but estimates of their global warming potential are often not available. These would, together with other safety and other environmental considerations, help assess the desirability of their use.

In this paper, first estimates are provided for 4 such alternatives: ethyl formate ($C_3H_6O_2$), cyanogen (C_2N_2), hydrogen cyanide (HCN) and phosphine (PH_3). Two essential inputs to GWP calculations are: (i) the radiative efficiency (RE), which is normally reported as the radiative forcing for a 1 ppb increase in the mole fraction of the gas, and requires information on the infrared absorption of the gas; and (ii) the atmospheric lifetime, which is needed for calculating the persistence of a pulse emission of a gas (as is assumed in the GWP framework); atmospheric lifetime also influences RE because it impacts the degree to which a gas is well mixed in the atmosphere after it has been emitted. The paper uses existing measurements of infrared absorption and reaction rate coefficients to provide new calculations of lifetimes, radiative efficiencies and global warming potentials (and other climate emission metrics).

2. Spectroscopic data

Radiative efficiency calculations (see section 3) require laboratory-measured or simulated absorption cross-sections at appropriate infrared wavelengths (wavelengths greater than 3.3 μm or wavenumbers from 0–3000 cm^{-1}). The prime source used here is the HITRAN2020 spectroscopic database (Gordon *et al* 2022 and https://hitran.org/) which is predominantly laboratory-based. HITRAN provides spectral data in two formats. One is via catalogues of individual spectral lines, henceforth referred to as 'line-by-line', and absorption cross-sections (Kochanov *et al* 2019), where individual vibrational transitions are not resolved. Most of the absorption cross-section data used here are measured cross-sections from the Pacific Northwest National Laboratory (PNNL) (Sharpe *et al* 2004; Johnson *et al* 2010).

In addition to the four gases of interest, SO_2F_2 is reconsidered to ensure consistency between the methodology used here and older results (e.g., Papadimitriou *et al* 2008).

In most cases, data is available at a range of temperatures. Generally, the integrated absorption cross-sections are relatively insensitive to temperature (e.g., Hodnebrog *et al* 2013, 2020), although there is some variation in the shape of spectral features with temperature. Given other uncertainties in calculating radiative efficiencies and GWPs, absorption cross-sections close to room temperature (296 to 298 K) are used here.

Absorption cross-sections, where available, are extracted or derived in the wavenumber range 0–3000 cm^{-1} covering the thermal infrared spectral region; this is consistent with most previous studies, and with listings in the Intergovernmental Panel on Climate Change Sixth Assessment Report (Forster *et al* 2021, Smith *et al* 2021). Any influence of these gases on the absorption of solar radiation (mostly at wavenumbers greater than 3000 cm^{-1}) would require a much more detailed study but is estimated to alter values by no more than 5%–10%; this estimate is based on the additional 7% forcing from absorption of solar radiation found by Byrom and Shine (2022) for the case of methane.

To calculate radiative efficiency (see section 4), cross-section data (which is typically measured at about 0.1 cm^{-1} spectral resolution) is averaged to a resolution of 1 cm^{-1}; it has units of cm^2 $molecule^{-1}$. The 0–3000 cm^{-1} integrated absorption cross-section is given in cm^{-1} $(molecule\ cm^{-2})^{-1}$. The absorption cross-section data for all the molecules studied here are presented in the bottom 5 frames of figure 1 and are also provided in the supplementary information at 1 cm^{-1} spectral resolution.

2.1. Sulfuryl fluoride

HITRAN2020 provides measured absorption cross-sections of SO_2F_2 from PNNL at wavenumbers 500–6500 cm^{-1} at 0.112 cm^{-1} resolution which were previously used in RE calculations (assuming the molecule to be well-mixed) by Hodnebrog *et al* (2020) (see table S6 of their supporting information). Measurements are made in the presence of nitrogen (N_2) at a pressure of 1 standard atmosphere (1013.25 hPa). The 298.15 K spectrum yields a 0–3000 cm^{-1} integrated absorption cross-section of 1.404×10^{-16} cm^{-1} $(molecule\ cm^{-2})^{-1}$. This agrees well with 1.396×10^{-16} cm^{-1} $(molecule\ cm^{-2})^{-1}$ measured by Papadimitriou *et al* (2008); this in turn agrees with Sulbaek Andersen *et al* (2009), although that work excludes the relatively weak absorption band peaking near 550 cm^{-1} (see figure 1).

2.2. Ethyl formate

HITRAN2020 provides measured absorption cross-sections of $C_3H_6O_2$ from PNNL at wavenumbers 500–6500 cm^{-1} at 0.112 cm^{-1} resolution which were previously used in RE calculations (assuming the molecule to be well-mixed) by Hodnebrog *et al* (2020) (see table S6 of their supporting information). Measurements are made in the presence of N_2 at a pressure of 1 standard atmosphere. The 298.15 K spectrum is used, yielding a 0–3000 cm^{-1} integrated absorption cross-section of 1.468×10^{-16} cm^{-1} $(molecule\ cm^{-2})^{-1}$.

2.3. Cyanogen

HITRAN2020 does not include an absorption cross-section file for C_2N_2. However, a PNNL spectrum was sourced from an author of the Sharpe *et al* (2004) study (Timothy J Johnson, PNNL, personal communication, 21 March 2022). This provides data at wavenumbers 575–6500 cm^{-1} at 0.112 cm^{-1} resolution at 298.15 K in the presence of N_2 at a pressure of 1 standard atmosphere. These data were provided in $\log_{10}$ 'absorbance' units; to derive absorption cross sections, these are first after converted to $\log_e$ and the resulting optical depth is then used to derive the absorption cross section using the stated path length of 2.142×10^{-6} grams/litre-metre (or equivalently 1 ppm-metre), which yields 2.48×10^{15} molecule cm^{-2}. The integrated cross-section at wavenumbers up to 3000 cm^{-1} is 1.684×10^{-18} cm^{-1} $(molecule\ cm^{-2})^{-1}$.

Cyanogen also has a very strong absorption band centred near 250 cm^{-1} (figure 1) which is not included in the PNNL data. Although this wavenumber region contributes relatively little to the radiative efficiency (see section 4), it was deemed important enough to include. This band is included in the HITRAN2020 line-by-line data. To

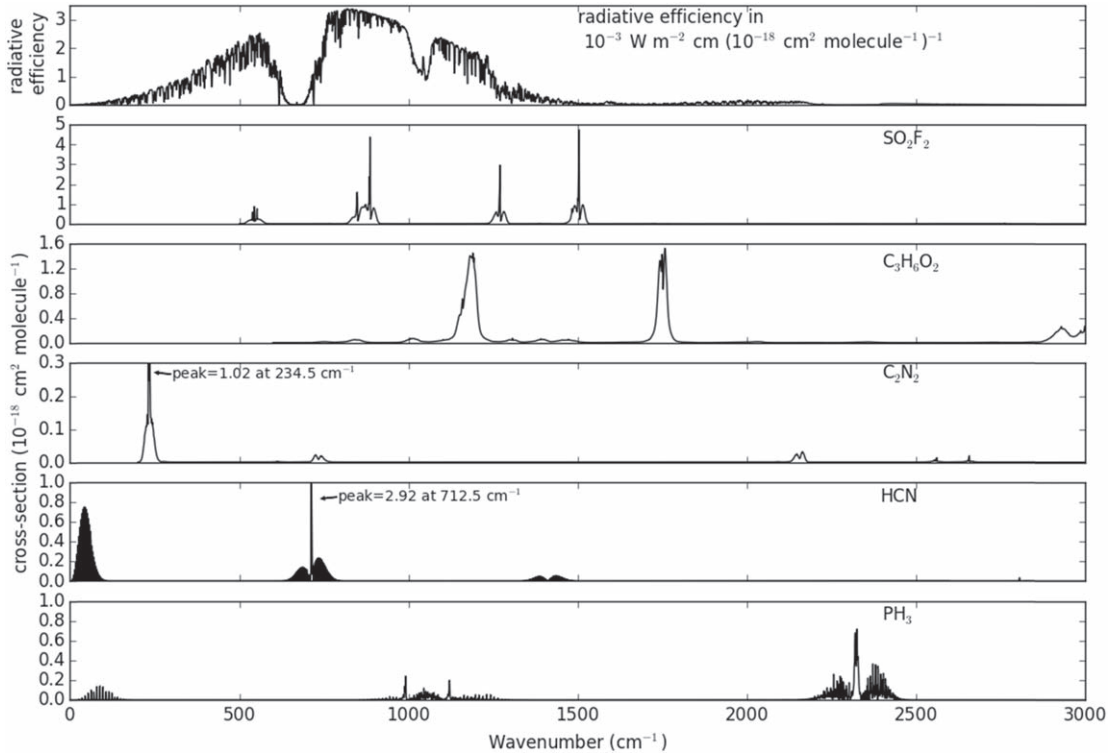

Figure 1. Top plot: Radiative efficiency of a weak absorber as a function of wavenumber (from Shine and Myhre 2020). The next 5 rows show the absorption cross-sections (at 296 K) at 1 cm^{-1} resolution, derived from observations as described in section 2, for SO_2F_2, $C_3H_6O_2$, C_2N_2, HCN and PH_3. Note the different vertical axes for the cross-section data.

generate cross-section data, line intensities at 296 K (in cm^{-1} (molecule $cm^{-2})^{-1}$) are summed over 1 cm^{-1} spectral intervals and then divided by the spectral interval to generate the required cross-sections in cm^2 $molecule^{-1}$. The integrated cross-section of this band is 6.140×10^{-18} cm^{-1} (molecule $cm^{-2})^{-1}$. Combining the PNNL and HITRAN data sources gives a total integrated cross-section of 7.824×10^{-18} cm^{-1} (molecule $cm^{-2})^{-1}$.

2.4. Hydrogen cyanide

HITRAN2020 does not include an absorption cross-section file for HCN. Instead, as for cyanogen, this molecule is included in the HITRAN2020 line-by-line data, and a similar procedure is used to generate cross-sections. The integrated cross-section at 296 K is 2.318×10^{-17} cm^{-1} (molecule $cm^{-2})^{-1}$. Hodnebrog *et al* (2020) report the integrated PNNL cross-section between 550 and 3000 cm^{-1} to be 1.4×10^{-17} cm^{-1} (molecule $cm^{-2})^{-1}$, which is about 10% higher than that derived from the HITRAN2020 line-by-line data for the same spectral interval (1.23×10^{-17} cm^{-1} (molecule $cm^{-2})^{-1}$).

2.5. Phosphine

Phosphine is also available in the HITRAN2020 line-by-line data and absorption cross-sections are generated in the same way as for cyanogen. The integrated cross-section at 296 K is 2.588×10^{-17} cm^{-1} (molecule $cm^{-2})^{-1}$.

3. Atmospheric lifetimes

We take the SO_2F_2 lifetime of 36 years from Gressent *et al* (2021) which is mainly due to ocean surface hydrolysis and reaction with OH. The tropospheric sink of HCN mainly results from a chemical reaction with OH, and its atmospheric lifetime is taken to be 0.5 years (e.g., Li *et al* 2009).

There do not appear to be recent assessments of the lifetimes of the other gases considered here. It is assumed that the dominant loss process is a reaction with OH, and lifetimes are estimated using the simple method (e.g., Orkin *et al* 2020 and references therein) which calibrates against the lifetime of methyl chloroform (MCF), where the lifetime of a molecule x, τ_x^{OH} is given by

$$\tau_x^{OH} = \frac{k_{MCF}(272\ K)}{k_x(272\ K)} \tau_{MCF}^{OH}.$$

τ_{MCF}^{OH} is the lifetime of MCF (taken to be 6 years) and $k_{MCF}(272\ K)$ and $k_x(272\ K)$ are the rate constants (at 272 K) of MCF and molecule x respectively. $k_{MCF}(272\ K)$ is taken to be 6.14×10^{-15} cm^3 molecule^{-1} s^{-1} from Burkholder *et al* (2019).

For ethyl formate, we use the 273 K rate constant estimate from Le Calvé *et al* (1997) of 8.9×10^{-13} cm^3 molecule^{-1} s^{-1}; this yields τ_{EF}^{OH} of 0.04 years or 15 days, in reasonable agreement with the 13.6 day estimate in Le Calvé *et al* (1997) based on an assumed typical tropospheric OH concentration of 10^6 molecule cm^{-3}. Balaganesh *et al* (2014) report measurements of the reaction of ethyl formate with chlorine atoms, which yields a lifetime of 3.5 years using global-average chlorine concentrations. Reaction with OH proceeds much faster than this and so the role of reaction with chlorine is not considered further here.

For cyanogen, less recent information seems available. Atkinson (1989) reports (on page 191) values of rate constant of $<3 \times 10^{-14}$ cm^3 molecule^{-1} s^{-1} which would imply a minimum lifetime of 1.22 years, close to that implied (without reference) by Purohit and Kumar (2021). Atkinson (1989) also reports measurements by Phillips (1979) in the temperature range of 300–550 K which gives a rate constant of $3.11 \times 10^{-13} \exp(-1448/T)$ cm^3 molecule^{-1} s^{-1} (where T is temperature in K) with an estimated error of 15%. Extrapolating to 272 K yields $k_{CY}(272\ K) = 1.5 \times 10^{-15}$ cm^3 molecule^{-1} s^{-1} which gives a lifetime τ_{EF}^{OH} of 24 years. Given the differences in these values, and the assumption that reaction with OH is the dominant atmospheric loss process, we use both 1.2 and 24 years in GWP_{100} calculations.

For phosphine, Atkinson (1989) (on page 203) reports a rate constant (measured between 249 and 438 K) of $2.7 \times 10^{-11} \exp(-155/T)$ cm^3 molecule^{-1} s^{-1} which gives $k_{PH}(272\ K) = 1.5 \times 10^{-11}$ cm^3 molecule^{-1} s^{-1} and hence τ_{PH}^{OH} of 2.4×10^{-3} years (about 0.9 days).

4. Radiative efficiencies

RE calculations use the Pinnock-curve methodology updated by Shine and Myhre (2020), where the RE of a weak absorber absorbing at all wavenumbers from 0 to 3000 cm^{-1} is calculated at 1 cm^{-1} resolution, in an atmosphere containing contemporary values of water vapour, carbon dioxide, ozone, nitrous oxide, methane and clouds. This spectrally-resolved RE is shown in the top frame of figure 1, which indicates the wavenumber regions where additional weak absorber could contribute most effectively to RE. It is assumed that background concentrations of the gases studied here are zero, or at least low enough that the RE is linear in concentration change. Multiplying this curve by the actual absorption cross-section of a given gas (as in the lower frames of figure 1) at the same spectral resolution, and summing over all wavenumbers, yields its RE in W m^{-2} ppb^{-1}. The updated method includes the effect of stratospheric temperature adjustment. The Hodnebrog *et al* (2013) simple method for accounting for gas lifetime is applied, which impacts on the horizontal and vertical distribution of an emitted gas. For gases removed through reaction with tropospheric OH, the RE is found by multiplying the constant mole-fraction RE by $\frac{a\tau^b}{(1+c\tau^b)}$ where a = 2.962, b = 0.9312, c = 2.994, d = 0.9302; it is applicable for $10^{-4} < \tau < 10^4$ years. Hodnebrog *et al* (2013, 2020) note that this correction depends on an assumed distribution of emissions; the RE and GWP are dependent on the distribution of emissions, especially for the short-lived gases considered here, and so the correction should be treated as approximate for such gases.

Table 1 shows both the constant mole-fraction and lifetime-corrected RE values, which follow expectations based on both the strength of the infrared absorption and the wavenumbers at which that absorption occurs. Sulfuryl fluoride and ethyl formate have by far the highest constant mole-fraction RE, with the other gases at least an order of magnitude smaller. However, the short lifetime of ethyl formate considerably reduces its RE when the lifetime correction is applied.

The constant mole-fraction RE for SO_2F_2 agrees well with the value of 0.222 W m^{-2} ppb^{-1} from Papadimitriou *et al* (2008) and the constant and lifetime-corrected values of 0.215 and 0.211 W m^{-2} ppb^{-1} (Hodnebrog *et al* 2020 - table S6), given the different choices of underlying spectral data. The constant mole-fraction RE for ethyl formate (0.13 W m^{-2} ppb^{-1}) agrees with Hodnebrog *et al* (2020 - table S15), as it should, given the commonality of the method and spectral data. The constant mole-fraction RE for hydrogen cyanide is slightly lower than the Hodnebrog *et al* (2020 - table S20) value (0.011 versus 0.012 W m^{-2} ppb^{-1}); this difference is within the uncertainties of the underlying spectroscopic data (see section 2). The constant mole-fraction value for cyanogen is considerably higher than Hodnebrog *et al* (2020 - table S17) value (0.0034 versus 0.001 W m^{-2} ppb^{-1}) because of our inclusion of the strong absorption band centred near 250 cm^{-1} (figure 1). Apart from SO_2F_2, we know of no previous assessments of the lifetime-corrected RE.

5. Global warming potentials and other emission metrics

The standard method for calculating GWP_{100} is adopted here (see section 8.SM.11.1 of Myhre *et al* 2013, which includes the method to convert RE from per molecule to per kg), with the absolute GWP_{100} for CO_2

Table 1. Atmospheric lifetimes, radiative efficiencies (for both constant mole fraction and lifetime-corrected mole fraction) and 100-year global warming potentials (GWP_{100}), relative to an equal mass emission of carbon dioxide. See section 3 for a discussion of the different values of cyanogen lifetime used here.

Fumigant gases	Atmospheric lifetime (years)	Radiative efficiency (constant mole fraction) (W m^{-2} ppb^{-1})	Lifetime-corrected Radiative Efficiency (W m^{-2} ppb^{-1})	GWP_{100}
Sulfuryl fluoride (SO_2F_2)	36	0.23	0.22	4630
Ethyl formate ($C_3H_6O_2$)	0.04	0.13	0.017	0.57
Hydrogen cyanide (HCN)	0.5	0.011	0.0065	7.6
Cyanogen (C_2N_2)	1.2–24	0.0034	0.0026–0.0033	3.8–96
Phosphine (PH_3)	0.0024	0.0012	0.00013	0.001

Table 2. Additional climate emission metrics, including the 20- and 500-year global warming potential (GWP_{20} and GWP_{500}), the 50- and 100-year global temperature change potential (GTP_{50} and GTP_{100}) and the 50- and 100-year combined GTP ($CGTP_{50}$ and $CGTP_{100}$ with units of years) which is presented only for gases with lifetimes shorter than 20 years. See section 3 for a discussion of the different values of cyanogen lifetime used here. GWP_{100} values are presented in table 1.

	GWP_{20}	GWP_{500}	GTP_{50}	GTP_{100}	$CGTP_{50}$	$CGTP_{100}$
Sulfuryl fluoride (SO_2F_2)	7750	1410	4270	1850	—	—
Ethyl formate ($C_3H_6O_2$)	2.1	0.16	0.11	0.10	59	69
Hydrogen cyanide (HCN)	28	2.2	1.5	1.3	790	930
Cyanogen (C_2N_2) 1.2 years	14	1.1	0.75	0.68	400	470
Cyanogen (C_2N_2) 24 years	200	28	72	26	—	—
Phosphine (PH_3)	0.002	0.0002	0.0001	0.0001	0.06	0.07

(89.5×10^{-15} W m^{-2} yr kg^{-1}) taken from Forster *et al* (2021). The small carbon-cycle correction used in Forster *et al* (2021) is not implemented here for the absolute GWP_{100} of the fumigant gases, as other uncertainties (see section 6) will dwarf this effect. Table 1 shows the results. All GWPs presented here are for the direct radiative impact of the gas on the radiation budget and do not include any indirect impacts on other radiatively-active species in the atmosphere via chemical reactions.

There are few previous sources to compare our values to. For SO_2F_2 Papadimitriou *et al* (2008) report a GWP_{100} of 4780 while Hodnebrog *et al* (2020—see table S6) report a value of 4880, and Smith *et al* (2021) report a value of 4630. These are within about 5% of the value (4630) in table 1. Any differences originate from different choices in the spectroscopic data and the absolute GWP of CO_2. The almost exact agreement between the present result and Smith *et al* (2021) is regarded as somewhat coincidental, although similar methods were used in their derivation.

Table 1 shows that the GWP_{100} of the four alternative fumigant gases to SO_2F_2 have much lower values. The highest of these (about 100) is for cyanogen, when its higher (24-year) lifetime is used; it is still only 2% of the value for SO_2F_2. For reference, the GWP_{100} of the fumigant methyl bromide is 2.4 (Smith *et al* 2021).

Whilst GWP_{100} is the most widely-used metric to produce CO_2-equivalent emissions for non-CO_2 gases, it is not the only such metric available. As discussed in Forster *et al* (2021) (see especially their Box 7.3), the Intergovernmental Panel on Climate Change refrains from recommending a particular emission metric 'because the appropriateness depends on the purposes for which gases and forcing agents are being compared'. We follow Forster *et al* (2021) in presenting metric values for two further time horizons of the GWP, GWP_{20} and GWP_{500}, using their absolute GWP values for CO_2 of 2.43×10^{-15} and 3.14×10^{-14} W m^{-2} yr kg^{-1} respectively. They present Global Temperature change Potentials (GTP) for two time horizons, GTP_{50} and GTP_{100} using absolute GTP values for CO_2 of 4.28×10^{-16} and 3.95×10^{-16} K kg^{-1} respectively. For gases with lifetimes less than 20 years, they also present a combined GTP (CGTP) which is the ratio of the absolute global temperature potential for a sustained step change in emissions of short-lived species divided by the absolute GTP for CO_2; as explained in Forster *et al* (2021) this is because of the similarity in the temperature response of a change in sustained emissions of a short-lived gas to a pulse emission of (the much longer lived) CO_2. CGTP, which has the units of years, uses the same absolute GTP values for CO_2 as given above. The Forster *et al* (2021) GTP and CGTP calculations use a two-term impulse-response function (IRF(t)) for temperature given by

$$IRF(t) = \sum_{1}^{2} \frac{c_j}{d_j} \exp\left(-\frac{t}{d_j}\right)$$

where t is the time in years, $c_1 = 0.444$ K (W m^{-2})$^{-1}$, $c_2 = 0.314$ K (W m^{-2})$^{-1}$, $d_1 = 3.424$ years and $d_2 = 285.004$ years.

Table 2 presents the values of these additional metrics, again without the small carbon cycle correction. The table emphasises the considerable impact, on the apparent CO_2-equivalence, that the choice of metric has.

6. Uncertainties

The many possible sources of uncertainty in RE calculations are discussed in detail by Hodnebrog *et al* (2013 and 2020) and by Forster *et al* (2021) and Smith *et al* (2021); this includes uncertainties of typically 5% each in the experimental absorption cross-sections, in radiative transfer calculations and in the specification of the atmospheric profile. The dominant uncertainty (around 20%) originates from assumptions about the vertical profile for gases with lifetimes of less than 5 years, which impacts 4 of the 5 gases presented here. The calculation of GWP_{100} and other emission metrics is also affected by lifetime uncertainties and uncertainties in the absolute metric values of CO_2.

Smith *et al* (2021) assess the uncertainty (expressed as the 5%–95% confidence interval) of the GWP_{100} of the relatively short-lived halocarbon HFC-32 (lifetime 5.4 years) to be 38%. It will certainly be higher for the shorter-lived gases discussed here, and a 50% uncertainty is tentatively assigned.

As noted in section 4, the GWPs, and other emission metrics, for short-lived species will be dependent on where (and even when) they are emitted. This impacts both the lifetime-correction to the RE and the lifetime used within the GWP calculation. Hodnebrog *et al* (2013) show that the RE lifetime correction for short-lived gases (0.2 years) emitted mostly in tropical regions is considerably smaller than the correction when they are emitted from mid-latitudes. This would, for example, increase the lifetime-corrected RE of hydrogen cyanide of 0.0065 W m^{-2} ppb^{-1} by around 30%.

7. Conclusions

A rounded assessment of the impact of using new fumigants in place of established ones requires consideration of their climate impact. This is most commonly achieved using the GWP_{100}; while GWP_{100} values are available for sulfuryl fluoride, no values were available for 4 other fumigants (cyanogen, hydrogen cyanide, ethyl formate and phosphine). This letter has provided the first values for these, by exploiting available measurements of their infrared spectra, and deriving lifetimes from the literature, or from literature assessments of their reaction rate coefficients with the principal atmospheric oxidant OH.

While recognising the many uncertainties in these new values, they demonstrate that on a per kg emission basis, these alternate fumigants have GWP_{100} values which are, at most, only around 2% of those of sulfuryl fluoride. These new estimates will enable informed assessments of the climate implications of the use of these fumigants, which would need to consider the equivalent release rates (for the same fumigant efficacy) of each gas, and the extent to which it is, in practice, mixed with other gases.

The principal uncertainty identified here is the atmospheric lifetime of the fumigant gases, particularly cyanogen. Further work could reduce these uncertainties, examine atmospheric removal paths other than reaction with OH, and explore the impact of the sensitivity of the GWP_{100} to where and when the gases are emitted.

Acknowledgments

Andrew Leaf and Matt Hall are thanked for providing information on the usage of fumigants and pointing to relevant prior work for various information. Timothy Johnson of PNNL is thanked for providing infrared absorption cross-sections of cyanogen. The reviewers are thanked for comments that led to improvements in the text.

Data availability statement

All data that support the findings of this study are included within the article (and any supplementary files).

ORCID iDs

Keith P Shine https://orcid.org/0000-0003-2672-9978
Yi Kang https://orcid.org/0000-0001-9850-3981

References

Atkinson R 1989 Kinetics and mechanisms of the gas-phase reactions of the hydroxyl radical with organic compounds *J. Phys. Chem. Ref. Data* (https://nist.gov/srd/journal-physical-and-chemical-reference-data-monographs-or-supplements) Monograph 1. Available from (accessed December 2022) ISBN 0883187205

Balaganesh M, Dash M R and Rajakumar B 2014 Experimental and computational investigation on the gas phase reaction of ethyl formate with Cl atoms *J. Phys. Chem.* **118** 5272–8

Burkholder J B *et al* 2019 Chemical kinetics and photochemical data for use in atmospheric studies *Evaluation No. 19* (Pasadena: JPL Publication 19-5, Jet Propulsion Laboratory) (http://jpldataeval.jpl.nasa.gov)

Byrom R E and Shine K P 2022 Methane's solar radiative forcing *Geophys. Res. Lett.* **49** e2022GL098270

Forster P *et al* 2021 The Earth's Energy Budget, Climate Feedbacks, and Climate Sensitivity *Climate Change 2021: The Physical Science Basis. Contribution of Working Group I to the Sixth Assessment Report of the Intergovernmental Panel on Climate Change* ed V Masson-Delmotte *et al* (Cambridge: Cambridge University Press) ch 8 pp 923–1054

Gordon I E *et al* 2022 The HITRAN2020 molecular spectroscopic database *J. Quant. Spectrosc. Radiat. Transf.* **277** 107949

Gressent A *et al* 2021 Growing atmospheric emissions of sulfuryl fluoride *Journal of Geophysical Research: Atmospheres* **126** e2020JD034327

Hodnebrog Ø, Aamaas B, Fuglestvedt J S, Marston G, Myhre G, Nielsen C J, Sandstad M, Shine K P and Wallington T J 2020 Updated global warming potentials and radiative efficiencies of halocarbons and other weak atmospheric absorbers *Rev. Geophys.* **58** e2019RG000691

Hodnebrog Ø, Etminan M, Fuglestvedt J S, Marston G, Myhre G, Nielsen C J, Shine K P and Wallington TJ T J 2013 Global warming potentials and radiative efficiencies of halocarbons and related compounds: a comprehensive review *Rev. Geophys.* **51** 300–78

Johnson T J, Profeta L T M, Sams R L, Griffith D W T and Yokelson R L 2010 An infrared spectral database for detection of gases emitted by biomass burning *Vib. Spectrosc.* **53** 97–102

Kochanov R V *et al* 2019 Infrared absorption cross-sections in HITRAN2016 and beyond: expansion for climate, environment, and atmospheric applications *J. Quant. Spectrosc. Radiat. Transf.* **230** 172–221

Le Calvé S, Le Bras G and Mellouki A 1997 Temperature dependence for the rate coefficients of the reactions of the OH radical with a series of formates *J. Phys. Chem.* **101** 5489–93

Li Q, Palmer P I, Pumphrey H C, Bernath P and Mahieu E 2009 What drives the observed variability of HCN in the troposphere and lower stratosphere? *Atmos. Chem. Phys.* **9** 8531–43

Myhre G *et al* 2013 Anthropogenic and natural radiative forcing *Climate Change 2013: The Physical Science Basis. Contribution of Working Group I to the Fifth Assessment Report of the Intergovernmental Panel on Climate Change* ed T F Stocker *et al* (Cambridge: Cambridge University Press) pp 659–740

Orkin V L, Kurylo M J and Fleming E L 2020 Atmospheric lifetimes of halogenated hydrocarbons: improved estimations from an analysis of modeling results *Journal of Geophysical Research: Atmospheres* **125** e2019JD032243

Papadimitriou V C, Portmann R W, Fahey D W, Mühle J, Weiss R F and Burkholder J B 2008 Experimental and theoretical study of the atmospheric chemistry and global warming potential of SO_2F_2 *J. Phys. Chem.* **112** 12657–66

Phillips L F 1979 Rate of reaction of OH radicals with cyanogen *Combust. Flame* **35** 233–6

Purohit L P and Kumar S 2021 Chapter 10 - Cyanogen: Risk assessment, environmental, and health hazard *Hazardous Gases* ed J Singh *et al* (New York: Academic Press) pp 115–125

Sharpe S W, Johnson T J, Sams R L, Chu P M, Rhoderick G C and Johnson P A 2004 Gas-phase databases for quantitative infrared spectroscopy *Appl. Spectrosc.* **58** 1452–61

Shine K P and Myhre G 2020 The spectral nature of stratospheric temperature adjustment and its application to halocarbon radiative forcing *Journal of Advances in Modeling Earth Systems* **12** e2019MS001951

Smith C, Nicholls Z R J, Armour K, Collins W, Forster P, Meinshausen M, Palmer M D and Watanabe M 2021 The Earth's energy budget, climate feedbacks, and climate sensitivity - supplementary material. in Climate Change 2021: the Physical Science Basis *Contribution of Working Group I to the Sixth Assessment Report of the Intergovernmental Panel on Climate Change* ed V Masson-Delmotte *et al* (Geneva: Intergovernmental Panel on Climate Change)

Sulbaek Andersen M P, Blake D R, Rowland F S, Hurley M D and Wallington T J 2009 Atmospheric chemistry of sulfuryl fluoride: reaction with OH radicals, Cl atoms and O_3, atmospheric lifetime, IR Spectrum, and global warming potential *Environmental Science & Technology* **43** 1067–70